Journal of Materials Chemistry A

Accepted Manuscript

This is an *Accepted Manuscript*, which has been through the Royal Society of Chemistry peer review process and has been accepted for publication.

Accepted Manuscripts are published online shortly after acceptance, before technical editing, formatting and proof reading. Using this free service, authors can make their results available to the community, in citable form, before we publish the edited article. We will replace this *Accepted Manuscript* with the edited and formatted *Advance Article* as soon as it is available.

You can find more information about *Accepted Manuscripts* in the Information for Authors.

Please note that technical editing may introduce minor changes to the text and/or graphics, which may alter content. The journal's standard Terms & Conditions and the Ethical guidelines still apply. In no event shall the Royal Society of Chemistry be held responsible for any errors or omissions in this *Accepted Manuscript* or any consequences arising from the use of any information it contains.

ROYAL SOCIETY OF CHEMISTRY

www.rsc.org/materialsA

Journal Name

ARTICLE

Three Dimensional Porous Graphene-Like Carbon Cloth from Cotton for a Free-Standing Lithium-Ion Battery Anode

Received 00th January 20xx,
Accepted 00th January 20xx

DOI: 10.1039/x0xx00000x

www.rsc.org/

Hui Bi,[a] Zhanqiang Liu,[a] Feng Xu,[a] Yufeng Tang,[a] Tianquan Lin[a] and Fuqiang Huang[*,a,b]

Most of carbon-based anodes have been reported to exhibit relatively low capacity due to the lack of superior electrical conductivity, mechanical flexibility and high electrochemical stability. Here, we report a new and simple approach to fabricate N-doped porous graphene-like carbon cloth from cotton cloth by using chemical vapor deposition. The N-doped carbon cloth has unique macroscopic hierarchy structure of few-layer graphene and super-high specific surface area of 1,890 $m^2 g^{-1}$, and exhibits outstanding mechanical and electrical characteristics. This free-standing carbon-based cloth is desirable to be an anode material in high power and energy density lithium ion batteries (LIBs). The N-doped carbon cloth shows a reversible capacity of 1,485 mAh g^{-1} at a current density of 50 mA g^{-1} after 80 charge-discharge cycles, which is nearly four times the theoretical capacity of graphite. More importantly, a very high capacity of ~500 mAh g^{-1} is obtained at 1.0 A g^{-1}, and fades less than 5% after 200 cycles, exhibiting excellent high-rate performance and long-term cycling stability. The N-doped carbon cloth is a superior flexible LIB anode to other carbon-based materials due to the good combination of hierarchy and porous structure, large surface area, high electrical conductivity and excellent mechanical stability.

Introduction

Sp^2 bonded carbon based materials exist in various types of allotropes, such as 0-dimensional fullerenes (0D C60), 1D carbon nanotubes (CNTs), and 2D graphene.[1] Graphite is considered as the 3D orderly stacked graphene, and has very good crystallite and excellent electrical conductivity, which can react with lithium following an intercalation/de-intercalation process to use as anode electrodes of lithium ion batteries (LIBs). However, the graphite material has low theoretical specific capacity (~372 mAh g^{-1}), and limited rate performance due to the slow chemical diffusion of lithium ions within the graphite electrode.[2, 3] Highly electrical conductive hard carbon has random alignment of graphene sheets which provides many voids to accommodate lithium to exhibit high reversible capacity (>500 mAh g^{-1}), but slow lithium ion diffusion makes hard carbon possess very poor rate capacity.[4, 5] Activated carbon is 3D porous material, and has a large amount of structrual defects and ultrahigh specific surface area (>3,000 $m^2 g^{-1}$), absorption of lithium ions on surface of activated carbon results in large first charge capacity, but very low Coulombic efficiency (<50%) due to the irreversible lithium loss during the intercalation/de-intercalation process.[6] Therefore, it remains a great challenge to develop the highly electrical conductivity and large specific surface area few-layer carbon nanostructure for the applications in LIB anodes.

To address these problems, graphene and CNT, due to good electrical conductivity, outstanding mechanical strength, low density and good flexibility, are considered as the most promising building blocks to explore novel free-standing, binder-free anodes for applications in LIBs. For example, flexible CNT films as LIB anodes exhibit a reversible charge of approx. 300 mAh g^{-1} with a stable cycling behavior.[7] Self-assembled graphene paper as a LIB anode exhibits the reversible capacity of as low as 84 mAh g^{-1} at a current rate of 50 mA g^{-1}.[8] Folded structured graphene paper exhibits an improved reversible capacitor of 568 mAh g^{-1} at 100 mA g^{-1} after 100 cycles.[9] Vertical array CNTs/graphene films have been constructed to exhibit a stable discharge capacity of 290 mAh g^{-1} at 30 mA g^{-1}, superior to the bare graphene films (~155 mAh g^{-1}).[10] In short, these self-assembled, free-standing, binder-free CNT and/or graphene anodes still exhibit relatively low capacity. In particular, their rate performances become poorer, and even the LIB devices cannot work at a high charge-discharge current.

In order to further improve the storage capacitance and rate performance, various strategies have been developed to-date, including designing nanostructured CNT and graphene,[11, 12] constructing porous, hollow and defect structures,[13-15] doping with heteroatoms such as B, N, *etc.*[14-17] Among the nanostructured carbon materials, N-doped carbon materials

[a] *State Key Laboratory of High Performance Ceramics and Superfine Microstructures and CAS Key Laboratory of Materials for Energy Conversion, Shanghai Institute of Ceramics, Chinese Academy of Sciences, Shanghai 200050, P.R. China. *Email - huangfq@mail.sic.ac.cn*
[b] *State Key Laboratory of Rare Earth Materials Chemistry and Applications and Beijing National Laboratory for Molecular Sciences, College of Chemistry and Molecular Engineering, Peking University, Beijing 100871, P.R. China.*
Electronic Supplementary Information (ESI) available: [details of any supplementary information available should be included here]. See DOI: 10.1039/x0xx00000x

This journal is © The Royal Society of Chemistry 20xx

Please do not adjust margins

Journal of Materials Chemistry A Accepted Manuscript

Please do not adjust margins

are attractive. For example, N-doped graphene with a 17.7 wt.% N content, as an anode material for LIB, outperforms a ultra-high capacity of over 2,132 mAh g^{-1} at a current density of 100 mA g^{-1}, and 785 mAh g^{-1} at 5.0 A g^{-1}.[17] However, due to high specific surface area of N-doped graphene, more amounts of polymer binder and conductive agent (~50 wt.% in the entire electrode) are necessary to firmly coat the anode electrode on a Cu current collector, which in turn lead to the reduced volumetric and gravimetric energy density to some extent. Although enormous research efforts have been made to construct the nanostructured carbon materials,[9, 18-22] it can be difficult to achieve the controllable and large scale fabrication of the nanostructured carbon materials with a good combination of proper pore size and/or number, N doping and some degree of graphitization. At the same time, it still remains larger challenge to self-assemble the nanostructured carbon materials for the formation of macroscopic free-standing flexible films with highly electrical conductivity, largely specific surface area and enhanced lithium storage capacity.

In this paper, we have demonstrated a novel N-doped porous graphene-like carbon cloth prepared by the one-step carbonization of commercial cotton cloth under NH_3 atmosphere. The porous carbon cloth has a free-standing flexible structure and large specific surface area, and exhibits an outstanding mechanical and electrical stability. More importantly, the N-doped carbon cloth acts as a binder-free anode electrode to deliver high specific capacity, excellent rate capability and superior cycling stability.

Experimental

Fabrication of 3D porous carbon

A piece of commercial cotton cloth was placed in the center of a horizontal quartz tube mounted inside a high-temperature furnace, then heated up to 900 °C under 50 sccm H_2 and 300 sccm Ar, and held at the reaction temperature for 1 h. In order to obtain N-doped graphene-like carbon cloth, a flow rate of 50 sccm NH_3 was also introduced at the elevated and reaction temperature, and H_2 and Ar gas flows were closed down. Finally, the sample was inserted into aqueous acid solution (the volume ratio of HF: H_3PO_4: HNO_3 = 1: 1: 1) for 12 h to remove the impurity, and further rinsed several times by deionized water and ethanol, and then dried in vacuum at 60 °C for 12 h.

LIB device preparation

Flexible, binder-free circular electrodes with a diameter of 14 mm were punched out from the free-standing porous carbon cloth. The electrodes were then dried at 120 °C in a vacuum chamber overnight. The CR2016 coin cells were then assembled in an argon-filled glove box using lithium metal as the cathode, a microporous glass-fiber membrane (Whatman) as the separator, and 1 M $LiPF_6$ (dissolved in ethylene carbonate and dimethyl carbonate with a 1:1 volume ratio) as the electrolyte.

Characterization and measurement

Morphology and structure were characterized with Field emission scanning electron microscope (FESEM, FEI Magellan 400), scanning transmission electron microscope (STEM), high resolution TEM (HRTEM, JEOL 2100F), energy-dispersive X-ray spectroscopy (EDS), electron energy loss spectroscopy (EELS), selected area electron diffraction (SAED), Raman spectra (Laser excitation energy of 532 nm), X-ray photoelectron spectroscopy (XPS, Thermo VG Scientific) and X-ray diffraction (XRD, Bruker D8). Specific surface area was obtained using nitrogen sorption measurements (ASAP 2020M, Micromeritics). Thermogravimetry (TG) and differential thermogravimetry (DTG) measurements (Thermoplus EVO II, Rigaku) were carried out at a heating rate of 10 °C min^{-1} in air. The electrical conductivities were measured by the Van der Pauw method with an Accent HL5500. The tensile tests were carried out by a single-column system (Instron-5566) with the loading capacity from 0.001 to 100 N at a constant loading speed of 2.0 mm min^{-1}. Cyclic voltammetry (CV) and electrochemical impedance spectroscopy (EIS) measurements were performed on a CHI 760E electrochemistry workstation. Charge-discharge characteristics were tested at various current densities of 50 mA g^{-1} to 10.0 A g^{-1} in the voltage range of 0–3.0 V on a CT2001A cell test instrument (LAND Electronic Co.) at room temperature.

Results and discussion

A piece of raw cotton cloth was pyrolyzed at 900 °C for 1 h to fabricate black and free-standing pristine porous carbon cloth (with H_2 and Ar gas flow) and N-doped porous graphene-like carbon cloth (with NH_3 gas flow), respectively. Compared with the raw cotton cloth, the porous carbon cloth suffers from great decrease in size due to the considerable removal of other components including oxygen and carbon species after the degradation of the cotton (Figure 1a). FESEM images (Figure 1b,c) show that the N-doped porous carbon cloth is a knit array of strands of a plurality of twisted carbon fibers with the diameters of 2.0–8.0 μm, and the morphology is similar to that of the pristine carbon cloth with larger fiber diameters (Figure S1). High magnification FESEM and STEM images (Figure 1d-f) show that the surface of carbon fibers is not smooth, and there are many mesoporous and macroporous voids inside carbon fibers, which are formed due to the evaporation of H_2O and CO_2 in the carbonization process and the removal of inorganic oxide nanoparticles. In order to confirm the element composition of the N-doped porous carbon cloth, the elemental mapping of EDS was obtained (Figure 1g-i), which is assigned to the elements C, O and N, respectively. Interestingly, the elemental mapping of these elements displays a very similar intensity distribution, revealing the effective incorporation and homogeneous distribution of a large quantity of N atoms into the skeletons of the porous carbon cloth.

Journal of Materials Chemistry A Accepted Manuscript

This journal is © The Royal Society of Chemistry 20xx

Please do not adjust margins

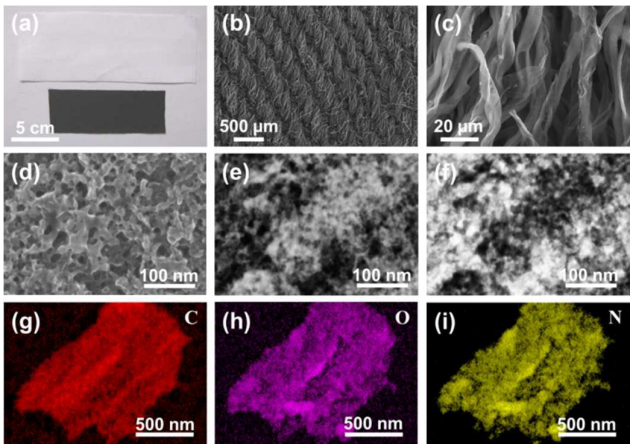

Figure 1. (a) Optical image of cotton and porous carbon cloths. (b, c) FESEM images of porous carbon cloth. (d-f) High-magnification FESEM and STEM images of porous carbon cloth. (g-i) Element mapping of N-doped porous carbon cloth for C, O and N elements.

TEM analyses were employed to investigate an individual carbon fiber. TEM electron beam is very difficult to penetrate through an individual carbon fiber of the pristine porous carbon cloth due to larger fiber diameter of the carbon fiber, compared with N-doped porous carbon cloth (Figure S2a), and HRTEM further confirms few voids inside the fiber (Figure S2b). The N-doped carbon fiber has twisted microstructure, and exhibits the semi-transparent characteristic under the electron beam of TEM (Figure 2a), indicating the high porosity of N-doped carbon fiber. Figure 2b further reveals the nanoporous structure inside the carbon fiber, and a ring-like SAED pattern confirms that the carbon fiber is graphitic and polycrystalline structure (Figure 2c), which is due to the presence of a large amounts of defective edges. HRTEM image (Figure 2d) shows that the carbon fiber is composed of a large amount of few-layer graphene sheets with the sizes of several nanometers, and the line profile (Figure 2e) exhibits that the *d*-spacing of the graphene sheets is in the range of 0.34–0.40 nm. The EELS spectrum from the carbon fiber shows two peaks at 284 eV and 291 eV (Figure 2f), which correspond to electron transitions from the 1*s* electronic states (or *K*-shell) to π^* and σ^* states, respectively, similar to the spectrum exhibited by graphite, confirming that the sp^2 bonds of the carbon fiber.[23]

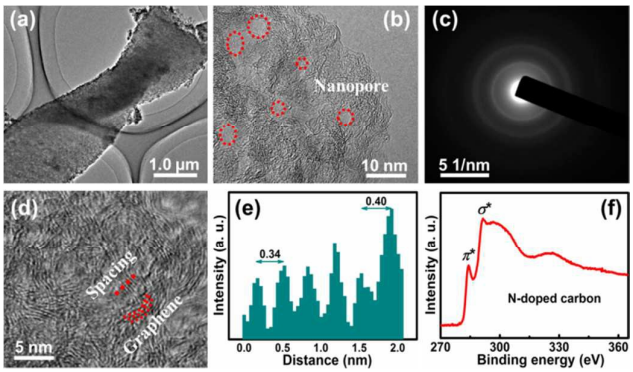

Figure 2. (a) TEM and (b) HRTEM images, (c) the SAED pattern, (d) high-magnification HRTEM image, (e) line profile of the *d*-spacing and (f) EELS spectrum of N-doped porous carbon cloth.

XRD spectra of the pristine and N-doped porous carbon cloths are shown in Figure 3a. The porous carbon cloths exhibit similar diffraction features with two broad peaks at 2θ=24° and 42°, indicating the typical of graphitic carbon material with some degree of graphitization.[17] Compared with the pristine porous carbon cloth, the broad peak at 2θ=24° of the N-doped porous carbon cloth shows slight shift to a larger angle, indicating that NH_3 treatment can remove the amorphous carbon and improve the crystalline quality of porous carbon cloth to some extent. Figure 3b shows the Raman spectra of the pristine and N-doped porous carbon cloths, displaying two prominent peaks of the D band and G band. Compared with the pristine porous carbon cloth, the D band and G band of N-doped porous carbon cloth upshifts, and the intensity ratio of D band to G band (I_D/I_G=1.42) slightly increases, suggesting the presence of a large amount of small graphene sheets and the structural distortion of porous carbon caused by the N heteroatoms introduction.[24, 25] The larger I_D/I_G and upshift of the D band and G band observed for the N-doped porous carbon cloth provides further evidence for the N doping in porous carbon cloth.

Journal of Materials Chemistry A Accepted Manuscript

This journal is © The Royal Society of Chemistry 20xx

Please do not adjust margins

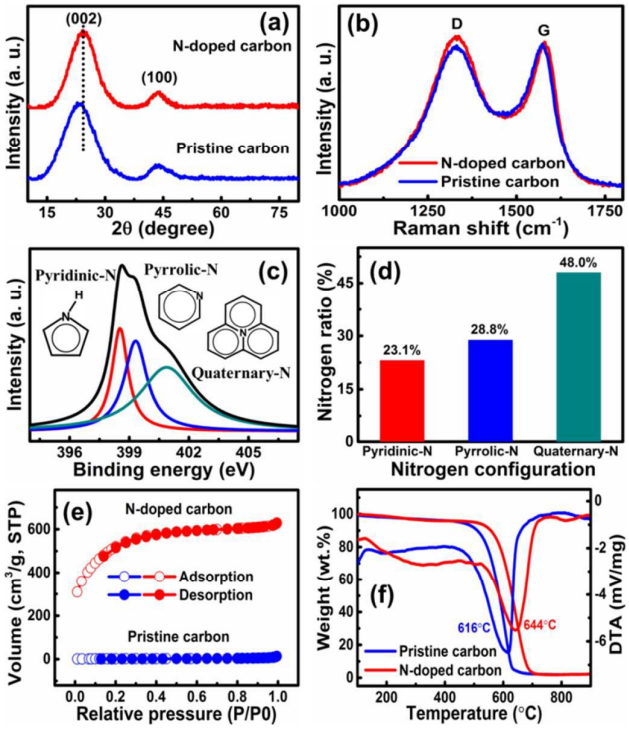

Figure 3. (a) XRD and (b) Raman spectra of pristine and N-doped porous carbon cloths. (c) N 1s XPS spectrum of N-doped porous carbon cloth. (d) The content of the pyridinic, pyrrolic and graphitic N atoms. (e) Adsorption-desorption isotherms and (f) TG/DTG curves of pristine and N-doped porous carbon cloths.

XPS measurements reveal that the N doping level is 10.9 at.% in the N-doped porous carbon cloth and 1.4 at.% in the pristine porous carbon cloth (Figure S3). In the XPS N1s spectrum of the N-doped porous carbon cloth, as shown in Figure 3c, three components represent pyridinic (N1, ~398.5 eV), pyrrolic (N2, ~399.3 eV), and graphitic (N3, ~400.9 eV) N atoms, respectively.[14, 16] The N binding configuration includes 23.1% pyridinic N, 28.8% pyrrolic N, and 48% graphitic N (Figure 3d). The N1s species in the N-doped porous carbon cloth can predominately supply much more chemically active sites to greatly increase the lithium storage capacity.

The nitrogen adsorption-desorption isotherms show that the specific surface area of the N-doped porous carbon cloth reaches up to 1,890 $m^2 g^{-1}$ (Figure 3e), which is much larger than that of the pristine porous carbon cloth (only 7.3 $m^2 g^{-1}$). The strong nitrogen adsorption below the relative to atmospheric pressure of 0.1 is characteristic of micropore filling, and the continuous rise of adsorption-desorption isotherms in the relative pressure range from 0.1 to 1.0 indicates the presence of mesopores (0.1–0.6) and macropores (0.6–1.0). The pore size distribution as determined by the Barret-Joyner-Halenda method shows that in the N-doped porous carbon cloth, much of the pore volume (0.49 cm^3/g) lies in the 1–10 nm range, with a double-peak pore diameter of 1.96 and 3.41 nm, respectively (Figure S4), consistent with the FESEM and HRTEM observations. Additionally, the N-doped porous carbon cloth shows a higher thermal stability of ~644 °C than that of the pristine porous carbon cloth (~616 °C) due to the simultaneous doping and removal of unstable carbon species during the doping process (Figure 3f).[16]

The N-doped porous carbon cloth has very good structural stability and flexibility, when the porous carbon cloth was folded up to almost 180° (Figure 4a). SEM image further verifies that the carbon fibers composed of porous carbon cloth still remain microstructural integrity, and almost no cracks occurs at a folding angle of ~180° (Figure 4b). Figure 4c shows that the porous carbon cloth exhibits a typical plastic deformation under tensile strength. In the elastic region, the porous carbon cloth has a typical Young's modulus of 5.3 MPa at a small deformation. Importantly, the porous carbon cloth is of high toughness with fracture elongation as high as 5.5%, and its fracture strength is measured to be 0.25 MPa.

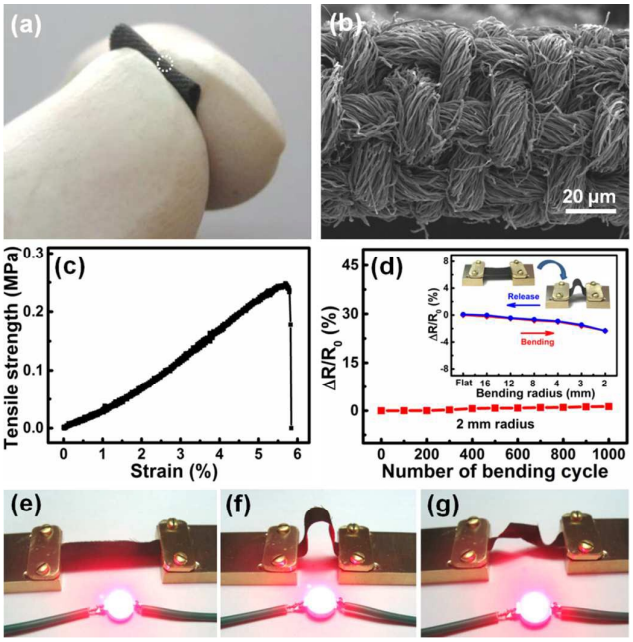

Figure 4. (a) Optical and (b) SEM images of porous carbon cloth with a 180° fold condition. (c) Typical mechanical measurement under tensile loading of porous carbon cloth at a strain rate of 2.0 mm min^{-1}. (d) The resistance change of porous carbon cloth under repeated bending cycles for a bend radius of 2.0 mm. Inset showing the electrical resistance change of porous carbon cloth for different bend radius. (e-g) Photographs of the devices for lightening a commercial LED using the porous carbon cloth with (e) the flat, (f) bending and (g) twisted situation.

Additionally, we further investigated the electrical property of the porous carbon cloth. The pristine porous carbon cloth has a sheet resistance of approx. 21.9 ohm sq^{-1}, and the corresponding electrical conductivity is approx. 318 S m^{-1}. After the N doping, the electrical conductivity decreases to 1.7 S m^{-1}, due to the introduction of a large amount of micropores, mesopores and structural defects/active sites inside the carbon fibers. When bending to a radius of 2.0 mm and then straightening for each cycle, the porous carbon cloth shows a small increase of ~2.8% in the electrical resistance. This resistance change is completely reversible by flattening back the porous carbon cloth to its original flat state

Journal of Materials Chemistry A Accepted Manuscript

This journal is © The Royal Society of Chemistry 20xx

Please do not adjust margins

(inset of Figure 4d). Moreover, only a slight change in resistance of less than 1.0% can be observed after 5,000 repeated bending cycles (Figure 4d). For direct demonstration, a red LED can be lit under 1.5 V circuit when directly connected with the porous carbon cloth use as a conductor (Figure 4e), indicating that the porous carbon cloth itself acts as an excellent electrical conductor. Moreover, the electronic circuits reveal almost no change in the LED brightness under various folding angles and twisting situations (Figure 4f,g). Therefore, the extraordinary electrical conductivity combined with the excellent mechanical robustness makes the porous carbon cloth an appropriate candidate for use as a flexible and stretchable electrode in energy storage and conversion devices.

The porous carbon cloth shows good mechanical flexibility and outstanding electrical property, thus we utilize it directly as both anode electrode and current collector of a LIB (Figure S5a). Figure 5a shows the galvanostatic voltage profiles of the N-doped porous carbon electrode at a current density of 50 mA g^{-1} in the voltage range 0–3.0 V versus Li^+/Li. At a current density of 50 mA g^{-1}, an ultrahigh initial discharge capacity of 3,365 mAh g^{-1} is recorded, and the charge capacity drops to 1,714 mAh g^{-1} in the first cycle. The Coulombic efficiency is more than 50%, and the capacity loss during the first cycle, which has been observed for many mesoporous carbon and graphene materials,[26, 27] is mainly attributed to the decomposition of electrolytes and the formation of a solid-electrolyte interface (SEI) on the porous carbon surface. The N-doped porous carbon cloth electrode still exhibits reversible capacity of 1,541 mAh g^{-1} after 10 cycles, over four times higher than those of the pristine porous carbon cloth (Figure 5b, ~233 mAh g^{-1} after 10 cycles), commercial carbon cloth (Figure S6, ~154 mAh g^{-1} after 10 cycles) and graphite (theoretical capacity: ~372 mAh g^{-1}). Such high specific capacity is also much superior to the free-standing and flexible CNT and graphene films,[3, 8-10, 22] and can be comparable to, even complete with the N-doped powder-like carbon-based active materials.[13-17]

Rate capability is an important factor for the use of LIBs in power applications. A good electrochemical energy storage device is required to provide its high energy density (specific capacitance) at a high charge-discharge current. The rate performance of the N-doped porous carbon cloth electrode is shown in Figure 5c. At high current densities of 500 mA g^{-1}, 1.0 A g^{-1}, 2.0 A g^{-1}, 5.0 A g^{-1} and 10.0 A g^{-1}, the reversible capacities of the N-doped porous carbon cloth reach up to 792 mAh g^{-1}, 500 mAh g^{-1}, 369 mAh g^{-1}, 183 mAh g^{-1} and 110 mAh g^{-1}, respectively, which are much higher than those of the pristine porous carbon cloth (~95 mAh g^{-1} at 1.0 A g^{-1}) and commercial carbon cloth (~56 mAh g^{-1} at 1.0 A g^{-1}). After 80 cycles at varied current densities, the capacity is retained at 1,485 mAh g^{-1} when the current density is reset to 50 mA g^{-1}. To further study the long-term stability of the N-doped porous carbon cloth electrode, the anode was continuously tested at 1.0 A g^{-1} for over 200 charge-discharge cycles. The capacity retention of the N-doped porous carbon anode at 1.0 A g^{-1} is as high as ~95.5% over 200 charge-discharge cycles, and the capacitor still reached up to 480 mAh g^{-1} (Figure 5d). The Columbic efficiency reaches up to >98%, indicating the excellent cycling stability.

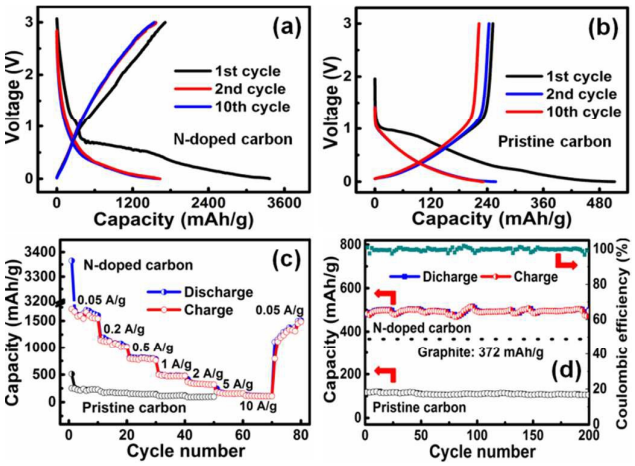

Figure 5. (a, b) Galvanostatic charge-discharge profile of N-doped and pristine porous carbon cloths at a current rate of 50 mA g^{-1} between 0 and 3.0 V for the initial 10 cycles. (c) Rate capabilities of pristine and N-doped porous carbon cloths obtained over a wide range of high current densities, from 50 mA g^{-1} to 10.0 A g^{-1}. (d) Cycle performance of pristine and N-doped porous carbon cloths obtained at a current density of 1.0 A g^{-1}.

To evaluate the possible use of the N-doped porous carbon cloth, we calculated their power and energy densities based on the single-electrode weight, as shown in Figure S7. For comparison, we also give the results for the pristine porous carbon cloth. It can be found that the N-doped porous carbon cloth delivers significantly higher energy and power densities than the pristine porous carbon cloth under fast charge-discharge rates. At a charge rate of 50 mA g^{-1}, the N-doped porous carbon cloth electrode delivers a maximum energy density of 2.9 kWh kg^{-1} with a power density of more than 78.8 W kg^{-1}. The fast charge-discharge capability in tens of seconds for the N-doped porous carbon cloth-based cells may tackle the power limitation of LIBs for high-power applications.

Due to outstanding mechanical property and structural integration, the porous carbon cloth can remain the almost same macro-morphology after the 200 charge-discharge cycles (Figure S5b), which can allow us to better investigate the reason why the N-doped porous carbon cloth electrode exhibits the excellent electrochemical properties. Firstly, the N-doped carbon cloth has much more micropores, mesopores and macropores (Figure 1 and 2) to act as electrochemical active sites to facilitate lithium ion diffusion into the inside of the graphene sheets. The CV curve of the N-doped porous carbon shows two reduction peaks of ~1.1 and 0.36 V in the first cycle (Figure 6a), which are ascribed to the irreversible reactions between the N-doped carbon cloth electrode and electrolyte and the co-intercalation of solvated lithium ions into graphene sheets.[14, 15] During the second cycle to the 10th cycle, there is no clear change, suggesting that the N-doped carbon cloth electrode is stable with reversible reactions during the following charge-discharge cycles (Figure 5a). Whereas the pristine carbon cloth electrode exhibits a reversible, sharp and intense peak at approx. 0.15 V vs. Li/Li^+, which is related to the de-intercalation of the lithium ion from the graphite materials (Figure S8). The unique kinetics and/or the mechanism of the reactions of the N-doped porous carbon cloth are entirely different to the pristine carbon cloth, which yields much increased specific capacity.[17]

Journal of Materials Chemistry A Accepted Manuscript

Additionally, the N doping greatly increases the electrochemical activity of the porous carbon cloth in the high-rate electrochemical process, which can be confirmed by the EIS measurements (Figure 6b). The Nyquist plots were modeled and interpreted with the help of an appropriate electric equivalent circuit (Inset of Figure 6b), and the electrolyte resistances (R_Ω) and charge transfer resistances (R_{CT}) have been estimated and listed in Table S1. It is revealed that the N-doped porous carbon cloth electrode shows the R_Ω of ~3.1 Ω, which is relatively lower than the identical electrode after 200 cycles, reflecting a good cycling stability of the N-doped carbon cloth electrode anode. This is in agreement with the discharge/charge measurements. Moreover, the R_{CT} of the N-doped carbon cloth electrode is about ~149.7 Ω before cycle, which substantially decreases down to 80.4 Ω after 200 cycles. This indicates that the lithium ion diffusion can be improved and the diffusion length can be reduced, thus making the N-doped porous carbon cloth suitable as lithium ion storage material even at high charge-discharge rates.

The defects and porous structure also give extra active sites for the storage of lithium ions, thereby greatly enhancing the electrode capacity of the N-doped carbon cloth. We further investigated the structural change of the N-doped porous carbon cloth after the electrochemical charge-discharge cycles, as shown in Figure 6c,d. It is clear that the porous carbon fiber still contains many defects and voids between discontinuous graphene sheets, similar to the carbon fiber before cycling, and microstructural and crystallinity of the N-doped porous carbon cloth does not obviously change after the charge-discharge cycles, confirmed by Raman and XRD spectra (Figure S9). In spite of repeated lithium ion insertion and extraction, the N-doped porous carbon cloth electrode is still able to retain its structural integrity, resulting in excellent electrochemical performance, including a high reversible capacity, excellent cycling stability and remarkable rate capability. Therefore, the N-doped carbon cloth electrode is a very promising candidate anode material for the next generation high performance LIBs.

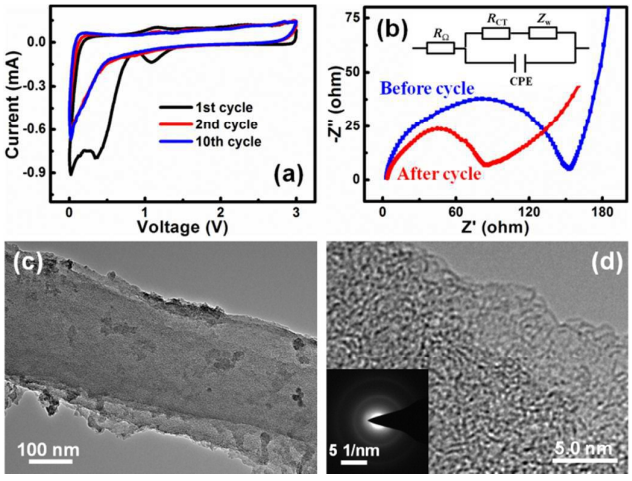

Figure 6. (a) CV curves for the initial 10 cycles. (b) Nyquist plots of N-doped porous carbon cloth before and after 200 charge-discharge cycles. Inset showing the modeled equivalent circuit of EIS. (c, d) TEM and HRTEM images of N-doped porous carbon cloth after 200 charge-discharge cycles. Inset showing the SAED pattern.

Conclusions

In summary, we have successfully developed a simple and scalable strategy for the preparation of N-doped porous carbon cloth by the carbonization of the cotton under NH_3 gas. The N-doped carbon cloth has a flexible macroscopic porous structure with a super-high specific surface area, and exhibits excellent mechanically robust and high electrical conductive properties. The prepared N-doped carbon cloth as a free-standing, binder-free anode electrode shows excellent electrochemical performance with a good combination of a high reversible specific capacity and a remarkable energy and power densities, outstanding rate capability, and long cycling stability. The novel fabrication method offers a pathway for realizing free-standing and high performance electrodes for energy storage and conversion devices.

Acknowledgements

Financial support from the NSF of China (Grant 61376056), Science and Technology Commission of Shanghai (Grants 13JC1405700 and 14520722000), Shanghai Science and Technology Development Funds (Grant 16QA1404200) and Key Research Program of Chinese Academy of Sciences (Grant KGZD-EW-T06), is acknowledged.

Notes and references

1 A. K. Geim and K. S. Novoselov, *Nature Mater.*, 2007, **6**, 183-191.
2 H. Bi, J. Chen, W. Zhao, S. Sun, Y. Tang, T. Lin, F. Huang, X. Zhou, X. Xie and M. Jiang, *RSC Adv.*, 2013, **3**, 8454-8460.
3 S. Zheng, Y. Chen, Y. Xu, F. Yi, Y. Zhu, Y. Liu, J. Yang and C. Wang, *ACS Nano*, 2013, **7**, 10995-11003.
4 H. Li, Z. Wang, L. Chen and X. Huang, *Adv. Mater.*, 2009, **21**, 4593-4607.
5 J. Ni, Y. Huang and L. Gao, *J. Power Sources*, 2013, **223**, 306-311.
6 C. H. Chen, R. Agrawal, Y. Hao and C. L. Wang, *J. Solid State Sci. Technol.*, 2013, **2**, 3074-3077.
7 S. Y. Chew, S. H. Ng, J. Wang, P. Novák, F. Krumeich, S. L. Chou, J. Chen and H. K. Liu, *Carbon*, 2009, **47**, 2976-2983.
8 A. Abouimrane, O. C. Compton, K. Amine and S. T. Nguyen, *J. Phys. Chem. C*, 2010, **114**, 12800-12804.
9 F. Liu, S. Song, D. Xue and H. Zhang, *Adv. Mater.*, 2012, **24**, 1089-1094.
10 S. Li, Y. Luo, W. Lv, W. Yu, S. Wu, P. Hou, Q. Yang, Q. Meng, C. Liu and H. M. Cheng, *Adv. Energy Mater.*, 2011, **1**, 486-490.
11 J. M. Shen and Y. T. Feng, *J. Phys. Chem. C*, 2008, **112**, 13114-13120.
12 Y. F. Luo, Y. Zhang, Y. Zhao, X. Fang, J. Ren, W. Weng, Y. S. Jiang, H. Sun, B. J. Wang, X. L. Cheng and H. S. Peng, *J. Mater. Chem. A*, 2015, **3**, 17553-17557.
13 Y. Fang, Y. Lv, R. Che, H. Wu, X. Zhang, D. Gu, G. Zheng and D. Zhao, *J. Am. Chem. Soc.*, 2013, **135**, 1524-1530.
14 Y. Chen, X. Li, K. Park, J. Song, J. Hong, L. Zhou, Y. W. Mai, H. Huang and J. B. Goodenough, *J. Am. Chem. Soc.*, 2013, **135**, 16280-16283.
15 Y. Chen, Z. Lu, L. Zhou, Y. W. Mai and H. Huang, *Energy Environ. Sci.*, 2012, **5**, 7898-7902.
16 Z. S. Wu, W. Ren, L. Xu, F. Li and H. M. Cheng, *ACS Nano*, 2011, **5**, 5463-5471.
17 F. Zheng, Y. Yang and Q. Chen, *Nature commun.*, 2014, **5**, 5261.

Journal of Materials Chemistry A Accepted Manuscript

This journal is © The Royal Society of Chemistry 20xx

Please do not adjust margins

18 X. Zhao, C. M. Hayner, M. C. Kung and H. H. Kung, *ACS Nano*, 2011, **5**, 8739-8749.
19 Z. J. Fan, J. Yan, T. Wei, G. Q. Ning, L. J. Zhi, J. C. Liu, D. X. Cao, G. L. Wang and F. Wei, *ACS Nano*, 2011, **5**, 2787-2794.
20 W. Wang, I. Ruiz, S. Guo, Z. Favors, H. H. Bay, M. Ozkan and C. S. Ozkan, *Nano Energy*, 2014, **3**, 113-118.
21 S. W. Lee, N. Yabuuchi, B. M. Gallant, S. Chen, B. S. Kim, P. T. Hammond and Y. Shao-Horn, *Nature Nanotech*, 2010, **5**, 531-537.
22 Z. Y. Pan, J. Ren, G. Z. Guan, X. Fang, B. J. Wang, S. G. Doo, I. H. Son, X. L. Huang and H. S. Peng, *Adv. Energy Mater.*, 2016, **6**, 1600271.
23 H. Bi, F. Huang, J. Liang, X. Xie and M. Jiang, *Adv. Mater.*, 2011, **23**, 3202-3206.
24 D. H. Seo, S. Kumar and K. Ostrikov, *Carbon*, 2011, **49**, 4331-4339.
25 H. Bi, W. Zhao, S. Sun, H. Cui, T. Lin, F. Huang, X. Xie and M. Jiang, *Carbon*, 2013, **61**, 116-123.
26 N. A. Kaskhedikar and J. Maier, *Adv. Mater.*, 2009, **21**, 2664-2680.
27 B. Guo, X. Wang, P. F. Fulvio, M. Chi, S. M. Mahurin, X. G. Sun and S. Dai, *Adv. Mater.*, 2011, **23**, 4661-4666.

Journal of Materials Chemistry A Accepted Manuscript

This journal is © The Royal Society of Chemistry 20xx

Please do not adjust margins

Graphical Abstract

Free-standing N-doped porous graphene-like carbon cloth has been fabricated as a lithium ion battery anode to deliver excellent electrochemical performance.

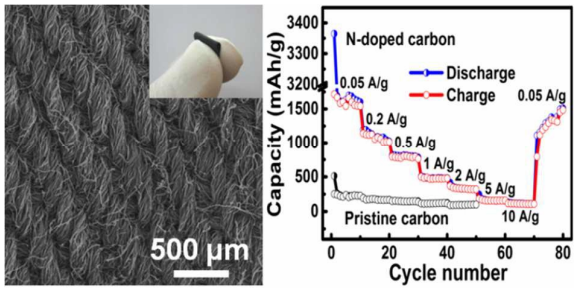

Journal of Materials Chemistry A Accepted Manuscript